**Proceedings of ASME Turbo Expo 2011**
**GT2011**
**June 6-10, 2011, Vancouver, British Columbia, Canada**

**GT2011-45341**

# METHOD TO EVALUATE SERVICE BOUNDARY CONDITIONS FOR GAS TURBINE STATOR STRUCTURE BY USING INVERSE ANALYSIS

**Y. HAYASAKA**
Hitachi, Ltd., Hitachi Research Laboratory,
Dept. for Material Research for Power Plants
3-1-1 Saiwai-cho, Hitachi-shi,
Ibaraki-ken, 317-8511 Japan
Email: yasushi.hayasaka.cp@hitachi.com

**M. SEKIHARA**
Hitachi, Ltd., Hitachi Research Laboratory,
Dept. for Material Research for Power Plants
3-1-1 Saiwai-cho, Hitachi-shi,
Ibaraki-ken, 317-8511 Japan

## ABSTRACT

*The service conditions and structures of gas turbines are so complex that it is very difficult to determine boundary conditions for thermal-mechanical analyses of these turbines. To improve the accuracy of the analyses, an analytical method for estimating the service boundary conditions for the whole gas turbine stator has been developed. This method consists of FEAs (finite element analyses), a DOE (design of experiments), and measured metal temperatures in an actual gas turbine. The FEAs, with varied boundary conditions, are analyzed using an orthogonal array. In each analysis, the differences between results of an FEA and the measured results are estimated. The model is modified to reduce the difference by using analyses of variance. The method was applied to a 150kW micro gas turbine stator and the good agreement between the analysis results and the measured data confirmed the validity of the method. The modified model is applied to the clearance setting and life assessment of the gas turbine.*

## INTRODUCTION

Gas turbine operating conditions are severe, especially for hot-gas-path components. The components are subjected to the conditions of thermal load, dynamic pressure oscillation, and environmental attack due to the high-temperature working fluid. To maintain the reliability of the turbine components, accurate structural analysis methods are desired(1). Furthermore, to improve the thermal efficiencies of the turbines, the turbine rotors and stator components have very small clearances to reduce leakage in spite of rubbing potential. From the clearance analysis point of view, accurate structural analysis methods are also required. On the other hand, the service boundary conditions of the high-temperature working fluid in gas turbines are so complex that it is very difficult to determine the boundary conditions for thermal-mechanical analyses of the turbines.

To improve the accuracy of the analyses, an analytical method for estimating the service boundary conditions for the whole gas turbine stator has been developed. This method uses an inverse analysis, which consists of FEAs (finite element analyses), a DOE (design of experiments), and measured metal temperatures in an actual gas turbine. The FEAs, with varied boundary conditions, are executed using an orthogonal array. In each analysis, the differences between the results of an FEA and the results of a measurement are estimated. The model is then modified to reduce the difference using an inverse analysis which applies analyses of variance iteratively.

For example, the method was applied to a 150kW micro-gas-turbine stator(2)(3). Using our proposed method, the average rate of errors was reduced from 15% to 9%. The good agreement between the analysis results and the measured data confirmed the validity of the method. The modified model is applied to the maintenance planning, life assessment, and clearance set of the gas turbine.

Our inverse analysis method has been used to estimate the thermal boundary conditions to improve the accuracy of the life assessment of hot-gas-path components(1). In this paper, the inverse analysis method was extended and applied to the life-assessment analysis and clearance analysis of a complete gas turbine structure. The method improves the accuracy of both analyses.

 

## METHOD FOR ESTIMATING SERVICE BOUNDARY CONDITIONS USING DOE

The flowchart of the method for estimating the service boundary conditions using DOE (design of experiments) is shown in Fig. 1. Firstly, we select the components to analyze. Then, the thermal and mechanical boundary conditions, which are calculated using computational fluid dynamics (CFD), are applied to the FEA models of the components.

To improve the accuracy of the FEA model, it is necessary to apply a service boundary condition, which describes the service conditions under a hot gas stream, to the model. Previous research shows that the service condition under a hot gas stream is so complex that many iterations were needed to determine it.

Therefore, the service boundary condition is estimated using DOE as shown in the flowchart enclosed in the bold box in Fig. 1. Firstly, the boundary conditions for multiple FEAs are arranged in an orthogonal array. The parameters of a component, such as temperature, stress, and strain, are analyzed by these FEAs. Then, using Equation (1), the analysis results derived from the FEAs are compared to the actual gas turbine data.

In Equation (1), $y$: the sum of squares of error; $T_a(k)$: the temperature derived from analysis; $T_{ins}(k)$: the temperature estimated from an actual gas turbine test or inspection; $k$: variable number. The boundary condition that minimizes $y$ in Equation (1) is determined to be the service boundary condition by using analyses of variance (ANOVA)[4].

$$y = \sum_{k=1}^{n_p} \{T_a(k) - T_{ins}(k)\}^2 \tag{1}$$

To apply our method to the entire micro gas turbine, Equation (1) is modified to Equation (2), because the whole micro gas turbine has a more complicated structure than the hot-gas-pass component. That is, the micro gas turbine consists of ten main components including a generator, a compressor and a turbine. Furthermore, the temperature differences of the components are up to about 1000K, because the temperature of the generator is about 310K, the temperature of the compressor is about 470K, and the temperature of the turbine is up to 1270K.

Therefore, in Equation (2), the temperature differences between the analysis results and the test results are estimated from their relative errors. The relative errors are averaged for all measuring points of each component. Finally, $y_{ave}$ is derived by averaging the relative errors for all components. In Equation (2), $m$: *the* component-number, $n_c$: the number of components, $n(m)$: the number of measuring points for the component $m$, $T_{am}(k)$: the temperatures of the component $m$ derived from analysis, $T_{im}(k)$: the temperatures of the component $m$ estimated by test, $k$: variable number.

$$y_{ave} = \frac{1}{n_c} \sum_{m=1}^{n_c} \left\{ \frac{1}{n(m)} \sum_{k=1}^{n(m)} \left( \frac{\left| T_{am}(k) - T_{im}(k) \right|}{T_{im}(k)} \right) \right\} \tag{2}$$

Next, using ANOVA [4], the boundary condition that minimizes $y_{ave}$ in Equation (2) is determined to be the service boundary condition. The equations of the analysis of variance are given in Equation (3). The boundary condition that reduces $y$ $(=y_{ave})$ is chosen by an F-test derived from ANOVA.

In this paper, two cases are presented and compared with each other. One is that only the boundary conditions whose significance levels are lower than 5% are changed. The other is that all the boundary conditions are changed to the level to reduce y without consideration of the significance level. The former case emphasizes statistical significance, and the latter case emphasizes increasing the number of the boundary conditions to reduce errors.

$$\begin{aligned}
S_T &= \sum_{i=1}^{l} \left( y_i - \bar{y} \right)^2 \\
S_j &= \sum_{k=1}^{n} a_{jk}^2 , \; a_{jk} = \bar{y}_{jk} - \bar{y} \\
S_e &= S_T - \sum_{j=1}^{m} S_j \\
V_j &= \frac{S_j}{f_j} \\
V_e &= \frac{S_e}{f_e} \\
F_j &= \frac{V_j}{V_e}
\end{aligned} \tag{3}$$

In Equation (3), $S_T$: the total sum of squares; $S_e$: the error sum of squares; $S_j$: the sum of squares for factor $j$; $f_j$: the degree of freedom of factor $j$; $f_e$: the degree of freedom of the error; $V_j$: the variance of factor $j$; $V_e$: the variance of the error; $F_j$: the F value.

The metal temperatures are then calculated for the chosen boundary conditions. The averaged relative error, $y_{ave}$, between the metal temperatures of the FEA with the service boundary conditions and the metal temperatures of the actual turbine are calculated and compared to a certain threshold, $y_{th}$. If the averaged relative error, $y_{ave}$, exceeds the threshold, $y_{th}$, the chosen boundary conditions are not estimated to be the service boundary conditions of the actual turbine. At that time, the steps to evaluate the service boundary conditions should be retraced, that is, the averaged relative error, $y_{ave}$, is reduced below the threshold, $y_{th}$, by reselecting the portion and parameter range of boundary conditions in the orthogonal array.

The FEA results under the service boundary condition are used for the clearance analysis and the life-assessment analysis. The service boundary conditions should improve the accuracy of both analyses. As a result, the reliability and efficiency of the gas turbines can be improved.

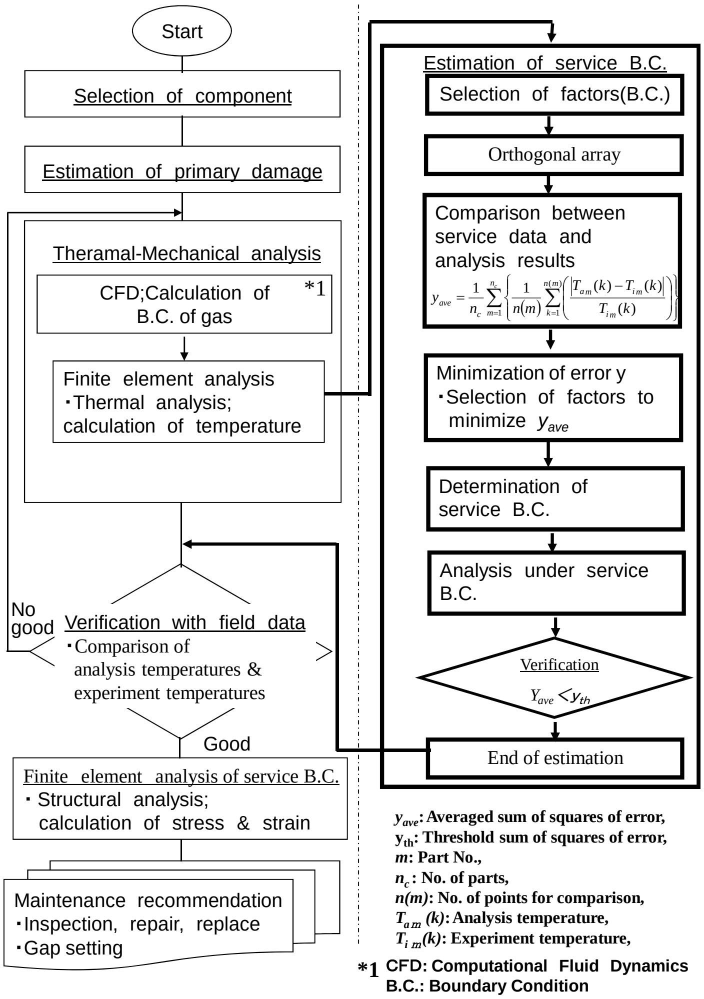


**Fig.1 Flow to estimate service boundary conditions**

## APPLICATION OF DEVELOPED METHOD TO A MICRO-GAS-TURBINE STRUCTURE

The method for estimating the service boundary conditions using DOE was applied to a 150kW micro gas turbine in order to validate its effectiveness following the flowchart shown in Fig.1.

### 150kW Micro-gas-turbine structure

The structure of a 150kW micro gas turbine is shown in Fig. 2. The micro-gas-turbine consists of a rotor, casings, a combustor, and a recuperator (not shown). The rotor, which consists of a permanent-magnet generator-rotor, a centrifugal compressor and a radial turbine, is supported by two water-lubricated bearings. The design specifications of the micro gas turbine are shown in Table 1[2][3].

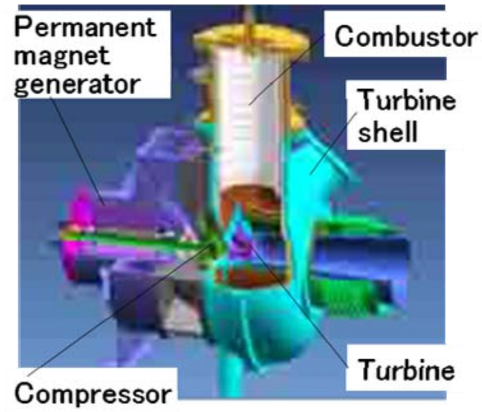


**Fig. 2 150kW micro-gas-turbine structure (Partially cut-model)**

**Table 1 Design specifications of micro gas turbine**

| Items | | Unit | Specification |
|---|---|---|---|
| Rated output | without WAC and HAT | kW | 129 |
| | with WAC and HAT | kW | 150 |
| Efficiency | without WAC and HAT | % | 32.5 |
| | with WAC and HAT | % | 35 |
| Rated rotational speed | | rpm | 51,000 |
| Compressor | Pressure ratio | - | 4 |
| | Adiabatic efficiency | % | 81 |
| Turbine | Inlet gas temperature | Deg. C | 960 |
| | Adiabatic efficiency | % | 85 |
| Combustor | NOx at 15% $O_2$ | ppm | $<$10 |
| Recuperator | Thermal efficiency | % | 92 |
| Bearings | Lubicant | - | Water |
| Generator | Efficiency | % | 95 |
| Power electronics | Efficiency | % | 92 |
| Noise | 1m point from the wall | dB | 65 |

WAC: Water Atomizing inlet Air cooling, HAT; Humid Air Turbine

### FEA model of 150kW micro-gas-turbine structure

A finite element model of the stator structure of the micro gas turbine is shown in Fig. 3. The finite element model has 200,000 nodes and 100,000 10-node tetrahedral elements of ANSYS11.0. The model is a whole gas-turbine-stator model which has almost the all the stator parts concerning clearance setting and life assessment. Therefore, the model avoids potential modeling errors, which sometimes occur in finite-element models divided into each component.

In temperature analyses, heat resistances at contact surfaces between the stator parts are not taken into account. In structure analyses, the meshes of the stator parts are connected at the nodes representing bolt locations.

The thermal boundary conditions, which consist of gas temperatures and heat transfer coefficients, are applied to the finite element model surfaces, which are exposed to combustion gases and cooling airs. The thermal boundary conditions were derived from a computational fluid-dynamics analysis (CFD) and heat-transfer engineering-formulas. The thermal boundary conditions at the compressor and the turbine were derived from the CFD analyses. For the turbine, the CFD code is CFX-TASCflow, which is a commercial code that solves the Raynolds averaged Navier-Stokes equations using the standard k-ε turbulence model[5]. The rest boundary conditions were calculated by the engineering formulas. Gas pressure was also used in the model as a mechanical boundary condition.

### Method for estimating service boundary conditions for the micro-gas-turbine structure

The fourteen gas temperatures and the twelve heat-transfer coefficients shown in Table 2 were selected as factors to be varied according to an orthogonal array. The regions which were considered to be significant under the thermal boundary condition were selected. The gas temperatures and heat transfer coefficients were varied by multiplying the initial values derived from the CFD analysis and engineering-formulas by the factors in Table 2.

All the factors except one were varied by three levels. For the heat-transfer coefficients, most of the factors were varied in the range from 0.5 to 1.5, because the heat-transfer coefficients can vary according to the accuracy of the calculation method such as the CFD and engineering-formulas[6]. It is because the heat-transfer coefficients can be affected by separated-flow, secondary-flow, vortex and windage due to complexity of the actual structure. The varying range was determined by our previous experiments[6]. The factors of for gas temperatures ranged from 0.8 to 1.2 because they were considered to have a good agreement to the actual gas temperatures. It is because the gas temperatures have a fewer uncertainties comparing to heat-transfer coefficients. In Table 2, some portions were assumed to be no-heat-crossing areas for the initial condition, for these portions, the 2$^{nd}$ levels were set as base levels. Finally, it is necessary to select the ranges appropriately considering the calculation method of the thermal boundary conditions and previous experiences. The ranges shown in Table 2 are considered to be acceptably small according to our knowledge.

Table 3 shows the L54 orthogonal array that we used in this paper. This array can vary 25 factors in 3-levels and 1 factor in 2-levels by 54 analyses.

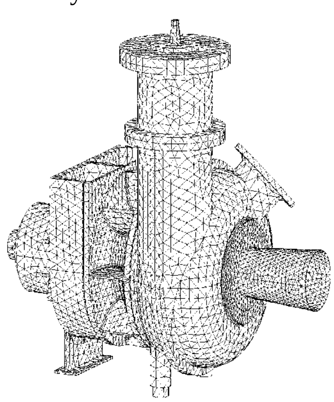

**Fig. 3 FEA model of micro-gas-turbine stator structure**

Analysis No. 1 in Table 3 means that the gas-temperatures and heat-transfer coefficients from Factor No. 1 to No. 26 are multiplied by one except for the heat-transfer coefficients from Factor No. 22 to No. 24 which are multiplied by zero because these portions were assumed to be adiabatic as previously mentioned.

**Table 2 Factors of temperatures and heat-transfer coefficients for FEAs**

| Factor No. | Thermal Baunday Conditions | Level | | |
|---|---|---|---|---|
| | | 1 | 2 | 3 |
| 1 | Gas TMP of Compressor Discharge Air | 1 | 1.1 | – |
| 2 | Gas TMP of Recuperator Outlet Air | 1 | 0.9 | 1.1 |
| 3 | Gas TMP of Turbine Exhaust Air | 1 | 1.1 | 1.2 |
| 4 | Metal TMP of Transition Piece of Combustor | 1 | 0.9 | 1.1 |
| 5 | Gas TMP of Turbine Nozzle Inlet Air | 1 | 0.9 | 1.1 |
| 6 | Gas TMP of Turbine Wheel Inlet Air | 1 | 1.1 | 1.2 |
| 7 | Gas TMP of Turbine Backplate Air | 1 | 1.1 | 1.2 |
| 8 | Gas TMP of Compressor Impeller's Back Surface Air (Outer) | 1 | 1.1 | 1.2 |
| 9 | Gas TMP of Compressor Impeller's Back Surface Air (Inner) | 1 | 1.1 | 1.2 |
| 10 | Gas TMP of Turbine Backplate Air (Outer) | 1 | 1.1 | 1.2 |
| 11 | Gas TMP of Turbine Backplate Air (Inner) | 1 | 1.1 | 1.2 |
| 12 | Gas TMP of Turbine Nozzle Outlet Air | 1 | 1.1 | 1.2 |
| 13 | Gas TMP of Turbine Shell at Exhaust | 1 | 1.1 | 1.2 |
| 14 | Gas TMP of Labyrinth Seal between Compressor & Turbine | 1 | 1.1 | 1.2 |
| 15 | HTC of Compressor Discharge Air | 1 | 0.5 | 1.5 |
| 16 | HTC of Recuperator Outlet Air | 1 | 0.5 | 1.5 |
| 17 | HTC of Turbine Exhaust Air | 1 | 0.5 | 1.5 |
| 18 | HTC of Turbine Nozzle Inlet Air | 1 | 0.5 | 1.5 |
| 19 | HTC of Turbine Wheel Inlet Air | 1 | 0.5 | 1.5 |
| 20 | HTC of Turbine Backplate Air | 1 | 0.5 | 1.5 |
| 21 | HTC of Compressor Impeller's Back Surface Air | 1 | 0.5 | 1.5 |
| 22 | HTC of Labyrinth Seal between Compressor & Turbine | 0 | 1 | 1.5 |
| 23 | HTC of Turbine Backplate Air (Outer) | 0 | 1 | 1.5 |
| 24 | HTC of Turbine Backplate Air (Inner) | 0 | 1 | 1.5 |
| 25 | HTC of Turbine Nozzle Outlet Air | 1 | 0.5 | 1.5 |
| 26 | HTC of Turbine Shell at Exhaust | 1 | 0.5 | 1.5 |
| TMP; Temperature | | | | |
| HTC; Heat Transfer Coefficient | | | | |

**Table 3 Orthogonal array L54 with 26 factors**

| No. | Factor No. | | | | | | | | | | | | | | | | | | | | | | | | | |
|---|---|---|---|---|---|---|---|---|---|---|---|---|---|---|---|---|---|---|---|---|---|---|---|---|---|---|
| | 1 | 2 | 3 | 4 | 5 | 6 | 7 | 8 | 9 | 10 | 11 | 12 | 13 | 14 | 15 | 16 | 17 | 18 | 19 | 20 | 21 | 22 | 23 | 24 | 25 | 26 |
| 1 | 1 | 1 | 1 | 1 | 1 | 1 | 1 | 1 | 1 | 1 | 1 | 1 | 1 | 1 | 1 | 1 | 1 | 1 | 1 | 1 | 1 | 1 | 1 | 1 | 1 | 1 |
| 2 | 1 | 1 | 1 | 1 | 1 | 1 | 1 | 1 | 2 | 2 | 2 | 2 | 2 | 2 | 2 | 2 | 2 | 2 | 2 | 2 | 2 | 2 | 2 | 2 | 2 | 2 |
| 3 | 1 | 1 | 1 | 1 | 1 | 1 | 1 | 1 | 3 | 3 | 3 | 3 | 3 | 3 | 3 | 3 | 3 | 3 | 3 | 3 | 3 | 3 | 3 | 3 | 3 | 3 |
| 4 | 1 | 1 | 2 | 2 | 2 | 2 | 2 | 2 | 1 | 1 | 1 | 1 | 1 | 1 | 2 | 3 | 2 | 3 | 2 | 3 | 2 | 3 | 2 | 3 | 2 | 3 |
| 5 | 1 | 1 | 2 | 2 | 2 | 2 | 2 | 2 | 2 | 2 | 2 | 2 | 2 | 2 | 3 | 1 | 3 | 1 | 3 | 1 | 3 | 1 | 3 | 1 | 3 | 1 |
| 6 | 1 | 1 | 2 | 2 | 2 | 2 | 2 | 2 | 3 | 3 | 3 | 3 | 3 | 3 | 1 | 2 | 1 | 2 | 1 | 2 | 1 | 2 | 1 | 2 | 1 | 2 |
| 7 | 1 | 1 | 3 | 3 | 3 | 3 | 3 | 3 | 1 | 1 | 1 | 1 | 1 | 1 | 3 | 2 | 3 | 2 | 3 | 2 | 3 | 2 | 3 | 2 | 3 | 2 |
| 8 | 1 | 1 | 3 | 3 | 3 | 3 | 3 | 3 | 2 | 2 | 2 | 2 | 2 | 2 | 1 | 3 | 1 | 3 | 1 | 3 | 1 | 3 | 1 | 3 | 1 | 3 |
| 9 | 1 | 1 | 3 | 3 | 3 | 3 | 3 | 3 | 3 | 3 | 3 | 3 | 3 | 3 | 2 | 1 | 2 | 1 | 2 | 1 | 2 | 1 | 2 | 1 | 2 | 1 |
| 10 | 1 | 2 | 1 | 1 | 2 | 2 | 3 | 3 | 1 | 1 | 2 | 2 | 3 | 3 | 1 | 1 | 1 | 1 | 2 | 3 | 2 | 3 | 3 | 2 | 3 | 2 |
| 11 | 1 | 2 | 1 | 1 | 2 | 2 | 3 | 3 | 2 | 2 | 3 | 3 | 1 | 1 | 2 | 2 | 2 | 2 | 3 | 1 | 3 | 1 | 1 | 3 | 1 | 3 |
| 12 | 1 | 2 | 1 | 1 | 2 | 2 | 3 | 3 | 3 | 3 | 1 | 1 | 2 | 2 | 3 | 3 | 3 | 3 | 1 | 2 | 1 | 2 | 2 | 1 | 2 | 1 |
| 13 | 1 | 2 | 2 | 2 | 3 | 3 | 1 | 1 | 1 | 1 | 2 | 2 | 3 | 3 | 2 | 3 | 2 | 3 | 3 | 2 | 3 | 2 | 1 | 1 | 1 | 1 |
| 14 | 1 | 2 | 2 | 2 | 3 | 3 | 1 | 1 | 2 | 2 | 3 | 3 | 1 | 1 | 3 | 1 | 3 | 1 | 1 | 3 | 1 | 3 | 2 | 2 | 2 | 2 |
| 15 | 1 | 2 | 2 | 2 | 3 | 3 | 1 | 1 | 3 | 3 | 1 | 1 | 2 | 2 | 1 | 2 | 1 | 2 | 2 | 1 | 2 | 1 | 3 | 3 | 3 | 3 |
| 16 | 1 | 2 | 3 | 3 | 1 | 1 | 2 | 2 | 1 | 1 | 2 | 2 | 3 | 3 | 3 | 2 | 3 | 2 | 1 | 1 | 1 | 1 | 2 | 3 | 2 | 3 |
| 17 | 1 | 2 | 3 | 3 | 1 | 1 | 2 | 2 | 2 | 2 | 3 | 3 | 1 | 1 | 1 | 3 | 1 | 3 | 2 | 2 | 2 | 2 | 3 | 1 | 3 | 1 |
| 18 | 1 | 2 | 3 | 3 | 1 | 1 | 2 | 2 | 3 | 3 | 1 | 1 | 2 | 2 | 2 | 1 | 2 | 1 | 3 | 3 | 3 | 3 | 1 | 2 | 1 | 2 |
| 19 | 1 | 3 | 1 | 2 | 1 | 3 | 2 | 3 | 1 | 2 | 1 | 3 | 2 | 3 | 1 | 1 | 2 | 3 | 1 | 1 | 3 | 2 | 2 | 3 | 3 | 2 |
| 20 | 1 | 3 | 1 | 2 | 1 | 3 | 2 | 3 | 2 | 3 | 2 | 1 | 3 | 1 | 2 | 2 | 3 | 1 | 2 | 2 | 1 | 3 | 3 | 1 | 1 | 3 |
| 21 | 1 | 3 | 1 | 2 | 1 | 3 | 2 | 3 | 3 | 1 | 3 | 2 | 1 | 2 | 3 | 3 | 1 | 2 | 3 | 3 | 2 | 1 | 1 | 2 | 2 | 1 |
| 22 | 1 | 3 | 2 | 3 | 2 | 1 | 3 | 1 | 1 | 2 | 1 | 3 | 2 | 3 | 2 | 3 | 3 | 2 | 2 | 3 | 1 | 1 | 3 | 2 | 1 | 1 |
| 23 | 1 | 3 | 2 | 3 | 2 | 1 | 3 | 1 | 2 | 3 | 2 | 1 | 3 | 1 | 3 | 1 | 1 | 3 | 3 | 1 | 2 | 2 | 1 | 3 | 2 | 2 |
| 24 | 1 | 3 | 2 | 3 | 2 | 1 | 3 | 1 | 3 | 1 | 3 | 2 | 1 | 2 | 1 | 2 | 2 | 1 | 1 | 2 | 3 | 3 | 2 | 1 | 3 | 3 |
| 25 | 1 | 3 | 3 | 1 | 3 | 2 | 1 | 2 | 1 | 2 | 1 | 3 | 2 | 3 | 3 | 2 | 1 | 1 | 3 | 2 | 2 | 3 | 1 | 1 | 2 | 3 |
| 26 | 1 | 3 | 3 | 1 | 3 | 2 | 1 | 2 | 2 | 3 | 2 | 1 | 3 | 1 | 1 | 3 | 2 | 2 | 1 | 3 | 3 | 1 | 2 | 2 | 3 | 1 |
| 27 | 1 | 3 | 3 | 1 | 3 | 2 | 1 | 2 | 3 | 1 | 3 | 2 | 1 | 2 | 2 | 1 | 3 | 3 | 2 | 1 | 1 | 2 | 3 | 3 | 1 | 2 |
| 28 | 2 | 1 | 1 | 3 | 3 | 2 | 2 | 1 | 1 | 3 | 3 | 2 | 2 | 1 | 1 | 1 | 3 | 2 | 3 | 2 | 2 | 3 | 2 | 3 | 1 | 1 |
| 29 | 2 | 1 | 1 | 3 | 3 | 2 | 2 | 1 | 2 | 1 | 1 | 3 | 3 | 2 | 2 | 2 | 1 | 3 | 1 | 3 | 3 | 1 | 3 | 1 | 2 | 2 |
| 30 | 2 | 1 | 1 | 3 | 3 | 2 | 2 | 1 | 3 | 2 | 2 | 1 | 1 | 3 | 3 | 3 | 2 | 1 | 2 | 1 | 1 | 2 | 1 | 2 | 3 | 3 |
| 31 | 2 | 1 | 2 | 1 | 1 | 3 | 3 | 2 | 1 | 3 | 3 | 2 | 2 | 1 | 2 | 3 | 1 | 1 | 1 | 1 | 3 | 2 | 3 | 2 | 2 | 3 |
| 32 | 2 | 1 | 2 | 1 | 1 | 3 | 3 | 2 | 2 | 1 | 1 | 3 | 3 | 2 | 3 | 1 | 2 | 2 | 2 | 2 | 1 | 3 | 1 | 3 | 3 | 1 |
| 33 | 2 | 1 | 2 | 1 | 1 | 3 | 3 | 2 | 3 | 2 | 2 | 1 | 1 | 3 | 1 | 2 | 3 | 3 | 3 | 3 | 2 | 1 | 2 | 1 | 1 | 2 |
| 34 | 2 | 1 | 3 | 2 | 2 | 1 | 1 | 3 | 1 | 3 | 3 | 2 | 2 | 1 | 3 | 2 | 2 | 3 | 2 | 3 | 1 | 1 | 1 | 1 | 3 | 2 |
| 35 | 2 | 1 | 3 | 2 | 2 | 1 | 1 | 3 | 2 | 1 | 1 | 3 | 3 | 2 | 1 | 3 | 3 | 1 | 3 | 1 | 2 | 2 | 2 | 2 | 1 | 3 |
| 36 | 2 | 1 | 3 | 2 | 2 | 1 | 1 | 3 | 3 | 2 | 2 | 1 | 1 | 3 | 2 | 1 | 1 | 2 | 1 | 2 | 3 | 3 | 3 | 3 | 2 | 1 |
| 37 | 2 | 2 | 1 | 2 | 3 | 1 | 3 | 2 | 1 | 2 | 3 | 1 | 3 | 2 | 1 | 1 | 2 | 3 | 3 | 2 | 1 | 1 | 3 | 2 | 2 | 3 |
| 38 | 2 | 2 | 1 | 2 | 3 | 1 | 3 | 2 | 2 | 3 | 1 | 2 | 1 | 3 | 2 | 2 | 3 | 1 | 1 | 3 | 2 | 2 | 1 | 3 | 3 | 1 |
| 39 | 2 | 2 | 1 | 2 | 3 | 1 | 3 | 2 | 3 | 1 | 2 | 3 | 2 | 1 | 3 | 3 | 1 | 2 | 2 | 1 | 3 | 3 | 2 | 1 | 1 | 2 |
| 40 | 2 | 2 | 2 | 3 | 1 | 2 | 1 | 3 | 1 | 2 | 3 | 1 | 3 | 2 | 2 | 3 | 3 | 2 | 1 | 1 | 2 | 3 | 1 | 1 | 3 | 2 |
| 41 | 2 | 2 | 2 | 3 | 1 | 2 | 1 | 3 | 2 | 3 | 1 | 2 | 1 | 3 | 3 | 1 | 1 | 3 | 2 | 2 | 3 | 1 | 2 | 2 | 1 | 3 |
| 42 | 2 | 2 | 2 | 3 | 1 | 2 | 1 | 3 | 3 | 1 | 2 | 3 | 2 | 1 | 1 | 2 | 2 | 1 | 3 | 3 | 1 | 2 | 3 | 3 | 2 | 1 |
| 43 | 2 | 2 | 3 | 1 | 2 | 3 | 2 | 1 | 1 | 2 | 3 | 1 | 3 | 2 | 3 | 2 | 1 | 1 | 2 | 3 | 3 | 2 | 2 | 3 | 1 | 1 |
| 44 | 2 | 2 | 3 | 1 | 2 | 3 | 2 | 1 | 2 | 3 | 1 | 2 | 1 | 3 | 1 | 3 | 2 | 2 | 3 | 1 | 1 | 3 | 3 | 1 | 2 | 2 |
| 45 | 2 | 2 | 3 | 1 | 2 | 3 | 2 | 1 | 3 | 1 | 2 | 3 | 2 | 1 | 2 | 1 | 3 | 3 | 1 | 2 | 2 | 1 | 1 | 2 | 3 | 3 |
| 46 | 2 | 3 | 1 | 3 | 2 | 3 | 1 | 2 | 1 | 3 | 2 | 3 | 1 | 2 | 1 | 1 | 3 | 2 | 2 | 3 | 3 | 2 | 1 | 1 | 2 | 3 |
| 47 | 2 | 3 | 1 | 3 | 2 | 3 | 1 | 2 | 2 | 1 | 3 | 1 | 2 | 3 | 2 | 2 | 1 | 3 | 3 | 1 | 1 | 3 | 2 | 2 | 3 | 1 |
| 48 | 2 | 3 | 1 | 3 | 2 | 3 | 1 | 2 | 3 | 2 | 1 | 2 | 3 | 1 | 3 | 3 | 2 | 1 | 1 | 2 | 2 | 1 | 3 | 3 | 1 | 2 |
| 49 | 2 | 3 | 2 | 1 | 3 | 1 | 2 | 3 | 1 | 3 | 2 | 3 | 1 | 2 | 2 | 3 | 1 | 1 | 3 | 2 | 1 | 1 | 2 | 3 | 3 | 2 |
| 50 | 2 | 3 | 2 | 1 | 3 | 1 | 2 | 3 | 2 | 1 | 3 | 1 | 2 | 3 | 3 | 1 | 2 | 2 | 1 | 3 | 2 | 2 | 3 | 1 | 1 | 3 |
| 51 | 2 | 3 | 2 | 1 | 3 | 1 | 2 | 3 | 3 | 2 | 1 | 2 | 3 | 1 | 1 | 2 | 3 | 3 | 2 | 1 | 3 | 3 | 1 | 2 | 2 | 1 |
| 52 | 2 | 3 | 3 | 2 | 1 | 2 | 3 | 1 | 1 | 3 | 2 | 3 | 1 | 2 | 3 | 2 | 2 | 3 | 1 | 1 | 2 | 3 | 3 | 2 | 1 | 1 |
| 53 | 2 | 3 | 3 | 2 | 1 | 2 | 3 | 1 | 2 | 1 | 3 | 1 | 2 | 3 | 1 | 3 | 3 | 1 | 2 | 2 | 3 | 1 | 1 | 3 | 2 | 2 |
| 54 | 2 | 3 | 3 | 2 | 1 | 2 | 3 | 1 | 3 | 2 | 1 | 2 | 3 | 1 | 2 | 1 | 1 | 2 | 3 | 3 | 1 | 2 | 2 | 1 | 3 | 3 |

Therefore Analysis No.1 is equivalent to the analysis whose boundary condition is the initial condition. For Analysis No. 2 in Table 3, the thermal boundary conditions from No.1 to No.8 in Table 2 are multiplied by the factor of level 1 in Table 2 and the thermal boundary conditions from No.9 to No.26 in Table 2 are multiplied by the factor of level 2 in Table 2. According to the orthogonal array shown in Table 3, 54 FEAs were executed.

## Measurement of temperatures of the micro gas turbine

We measured the metal temperatures of the micro gas turbine. Thermocouples were installed on components of the micro-gas-turbine stator structures. Examples of thermocouples on the outside surface of a turbine shell are shown in Fig. 4. They were spot-welded and covered with thin stainless sheets on the turbine shell. The thermocouples were also installed inside the casings. The total number of the thermocouples was about 70.

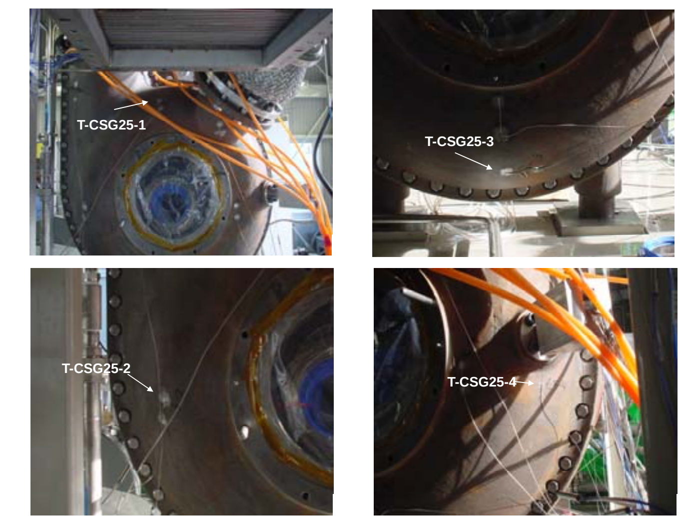


**Fig. 4 Thermocouples on the turbine shell**

## Identification of the service boundary conditions of the micro gas turbine

Next, by comparing the temperature measured by the thermocouples under steady-state operating condition and the temperature derived from FEA, the service boundary conditions were determined. The boundary condition that minimized $y_{ave}$ in Equation (2) was determined to be the service boundary condition. To determine the service boundary condition means to choose the level of each factor in Table 2 considering the significance level of each factor using the ANOVA shown in Equation (3).

The factor's effects on reducing $y_{ave}$ are shown in Fig. 5 and Fig. 6. The effects of the gas temperatures are shown in Fig. 5 and the effects of the heat-transfer coefficients are shown in Fig. 6. Setting the significance level at 5%, Factor 14 in Fig. 5, which is the gas temperature at a labyrinth seal between the centrifugal compressor and the radial turbine, is significant for reducing $y_{ave}$. Factor 23 in Fig. 6, which is the heat-transfer coefficient at a turbine back-plate, is also significant for reducing $y_{ave}$. Both factors are effective at reducing $y_{ave}$, as shown in Fig.5 and Fig.6.

Both significant factors are the boundary conditions which are located between back-to-back radial turbine wheel and centrifugal compressor. It is difficult to accurately estimate these boundary conditions because it is difficult to estimate the degree of air leakage between the back-to-back radial turbine wheel and centrifugal compressor. Therefore, our method indicated these boundary conditions should be corrected.

Factors 14 and 23 were chosen to minimize $y_{ave}$, thus giving a service boundary condition No. 55. For service boundary condition No. 56, all the factors were set to the levels to reduce $y_{ave}$. In service boundary condition No. 56, we value the number of factors more than statistical rigidity. The factors for the service boundary conditions are shown in Table 4.

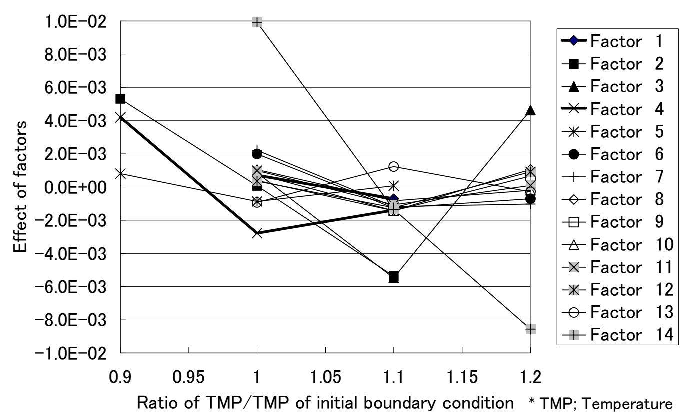


**Fig. 5 Effect of factors (TMP) reducing average relative error**

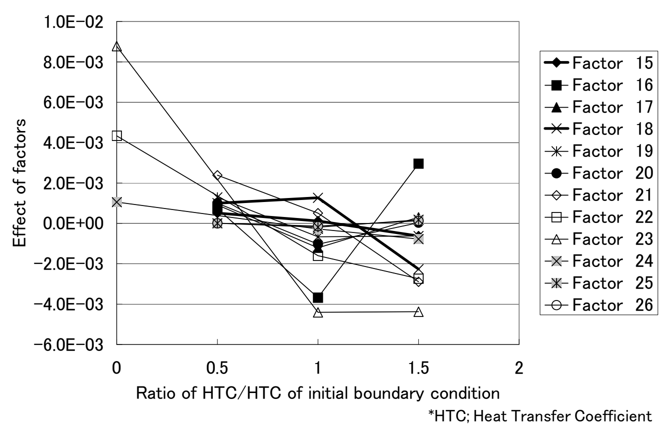


**Fig. 6 Effect of factors (HTC) reducing average relative error**

**Table 4 Factors for service boundary conditions**

| No. | Factor No. | | | | | | | | | | | | | | | | | | | | | | | | | |
|---|---|---|---|---|---|---|---|---|---|---|---|---|---|---|---|---|---|---|---|---|---|---|---|---|---|---|
| | 1 | 2 | 3 | 4 | 5 | 6 | 7 | 8 | 9 | 10 | 11 | 12 | 13 | 14 | 15 | 16 | 17 | 18 | 19 | 20 | 21 | 22 | 23 | 24 | 25 | 26 |
| 55 | 1 | 1 | 1 | 1 | 1 | 1 | 1 | 1 | 1 | 1 | 1 | 1 | 1 | 3 | 1 | 1 | 1 | 1 | 1 | 1 | 1 | 1 | 2 | 1 | 1 | 1 |
| 56 | 2 | 3 | 2 | 1 | 1 | 2 | 2 | 2 | 2 | 2 | 2 | 2 | 1 | 3 | 3 | 1 | 1 | 3 | 1 | 1 | 3 | 3 | 2 | 3 | 1 | 1 |

## Results of FEA under service boundary conditions

The relative errors, $y_{ave}$, of the FEAs under the service boundary conditions (No. 55, No. 56) are shown in Fig. 7. In this figure, the error, $y_{ave}$, of the analyses according to the orthogonal array are also plotted (from No. 1 to No. 54). Particularly, Analysis No.1 from the orthogonal array is under the initial boundary condition, which was derived from the CFD analysis and engineering formulas.

As shown in Fig. 7, $y_{ave}$ was 15% at No. 1 and decreased to 11% at No. 55 which changed the factors whose significance level was 5%. Under condition No. 56, in which all the factors were changed, $y_{ave}$ decreased to 9%. As the threshold, $y_{th}$, was set to 10% in the flowchart shown in Fig. 1, condition No. 56 was determined as the service boundary condition of the micro-gas-turbine stator structure.

Additionally, it is useful to find a relationship between the significance level and effect in order to reduce the relative error, $y_{ave}$. As shown in Fig. 7, it was important to change more than just the factors which were statistically significant in this case. Our extra investigation showed that the optimal number of factors to change was indicated by the said relationship.

A comparison between the metal temperature at the turbine back-plate derived from the FEA and the measured metal temperature is shown in Fig. 8. The vertical axis represents the metal temperature and the horizontal axis represents the firing temperature. The large solid symbols indicate the FEA results of service boundary condition No. 56, and the large open symbols indicate the FEA results of the initial boundary condition No. 1. The small solid symbols indicate the measured metal temperatures in the firing tests.

As shown in Fig. 8, the FEA results under service boundary condition No. 56 agree with the measured temperatures better than those under the initial condition (Condition No. 1). The difference between the FEA results and the measured temperatures dropped from between 100 and 200K to very small amount as the service boundary condition was applied. The differences in the other portions, which are not shown because of space limitations, were also reduced to small values by using this method.

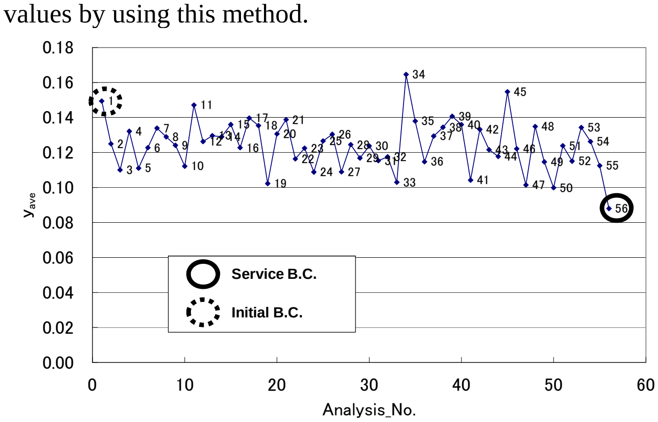


**Fig. 7 Effect of service B.C. on reducing error $y_{ave}$**

The modified model was applied to a clearance analysis and life assessment. For the clearance analysis, 2D FEM model for the whole micro gas turbine rotor and 3D FEM models for the compressor impeller and the turbine wheel were used. The clearance analysis under the service boundary condition can predict thermal deformation accurately so it is very effective to set the clearance between the compressor wheel, the radial turbine wheel, and the stator structures. For life assessment, the lives of the components were confirmed using the modified model, and some minor change was made for the component whose temperature was higher than initially predicted.

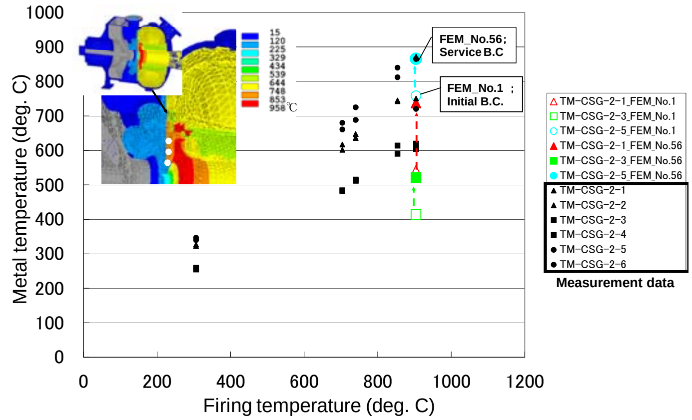


**Fig.8 Comparison between FEA and measurement**

## SUMMARY


To improve the accuracy of the clearance analysis and life assessment of a gas turbine, an analytical method for estimating the service boundary conditions was developed using inverse analysis with design of experiments.

The method was validated on a 150kW micro gas turbine. That is, the service boundary condition reduced the relative error, $y_{ave}$, from 15% to 9% and there was good agreement between the analysis results and the measured temperatures of the actual gas turbine. The modified model was applied to a clearance analysis and life assessment.


## REFERENCES


(1) Hayasaka, Y., Sakurai, S., and Takehara, I., Life Assessment Technology Using a Design of Experiments for Hot-gas-path Components of Gas Turbine, *Transactions of the Japan Society of Mechanical Engineers, Series A*, Vol. 68, No. 671 (2002-7), pp. 145-150.

(2) Dodo, S., Nakano, S., Inoue, T., Ichinose, M., Yagi, M., Tsubouchi, K., Yamaguchi, K., and Hayasaka, Y., Development of an Advanced Microturbine System Using Humid Air Turbine Cycle, *GT-2004-54337, ASME Turbo Expo, Vienna, Austria*, (2004-6).

(3) Nakano, S., Kishibe, T., Araki, H, Yagi, M., Tsubouchi, K., Ichinose, M., Hayasaka, Y., Ichinose, M., Sasaki, M., Inoue, T., Yamaguchi, K., and Shiraiwa, H., Development of a 150 kW Microturbine System Which Applies the Humid Air Turbine Cycle, *GT-2007-28192, ASME Turbo Expo, Montreal, Canada*, (2007-5).

(4) Taguchi, G, Design of Experiment, (1976), pp.330-338, Maruzen.

(5) M., Yagi, T., Kishibe, H., Tamaki and S., Nakano, *IGTC2007-ABS-114*.

(6) Kawaike K., Proc. Int. Sym. Heat Transfer in Turbomachinary, Greece,(August-1992), pp.73-84